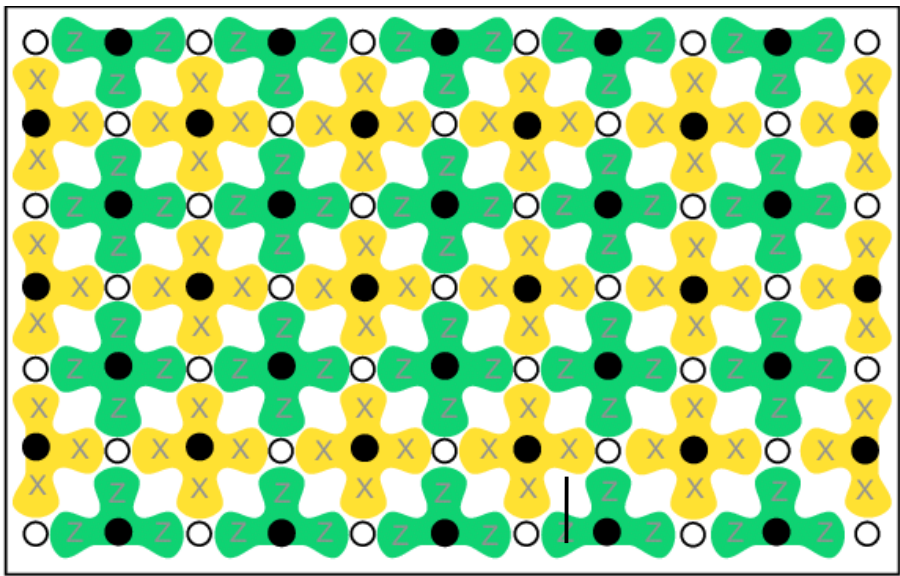
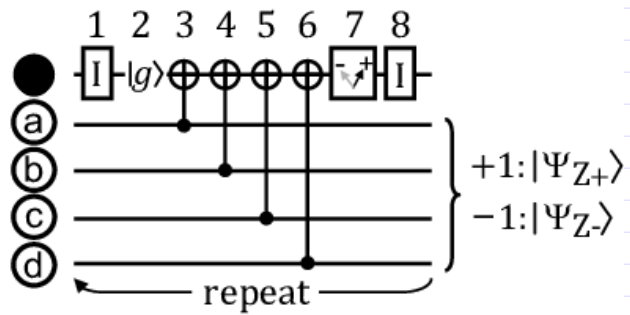
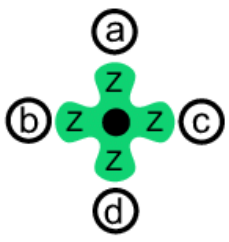


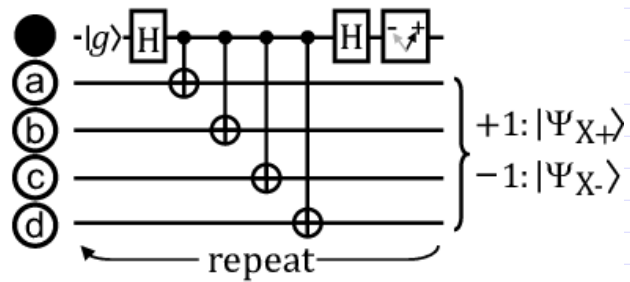
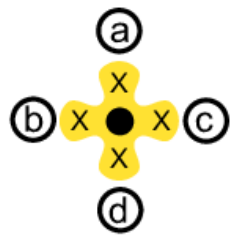
This will all be one logical qubit



(b)



(c)



arXiv: 1208.0928

Each measurement reduces the dimension of the Hilbert space by a factor of 2.

Start with $4 \cdot 6 + 3 \cdot 5 = 39$ data qubits so 2^{39} dim space.

But $4 \cdot 5 + 3 \cdot 6 = 38$ measurement qubits so $2^{39} / 2^{38} = 2$
 $\Rightarrow 1$ logical qubit

For example, 2 qubits

$|00\rangle |01\rangle |10\rangle |11\rangle$

measure $z_0 z_1 = +1 \Rightarrow |00\rangle, |11\rangle$

$= -1 \Rightarrow |01\rangle, |10\rangle$

Joint eigenstates of
 $z_0 z_1$, $x_0 x_1$ (they commute)

$z_0 z_1$ $x_0 x_1$

1

1

$$\frac{1}{\sqrt{2}} (|00\rangle + |11\rangle)$$

1

-1

$$\frac{1}{\sqrt{2}} (|00\rangle - |11\rangle)$$

-1

1

$$\frac{1}{\sqrt{2}} (|01\rangle + |10\rangle)$$

-1

-1

$$\frac{1}{\sqrt{2}} (|01\rangle - |10\rangle)$$

"Bell Basis"

For 4 qubits, there are eight $Z_a Z_b Z_c Z_d = +1$ eigenstates:

$|0000\rangle, |0011\rangle, \dots, |1100\rangle, |1111\rangle$
(all with even # of 1's)

Similarly, eight $Z_a Z_b Z_c Z_d = -1$ eigenstates:

$|0001\rangle, |0010\rangle, \dots, |1101\rangle, |1110\rangle$
(all with odd # of 1's)

Same for $X_a X_b X_c X_d$ in terms

$$| \pm \rangle = \frac{1}{\sqrt{2}} (|0\rangle \pm |1\rangle)$$

+1 $|++++\rangle, |++--\rangle, \dots, |--++\rangle, |----\rangle$

-1 $|+++-\rangle, |--+-\rangle, \dots, |--+-\rangle, |----\rangle$

Now consider error syndromes

$$Z_a Z_b Z_c Z_d X_a |\psi\rangle$$

error
on qubit a

$$= -X_a Z_a Z_b Z_c Z_d |\psi\rangle = -X_a |\psi\rangle$$

(if started in +1 eigenstate)

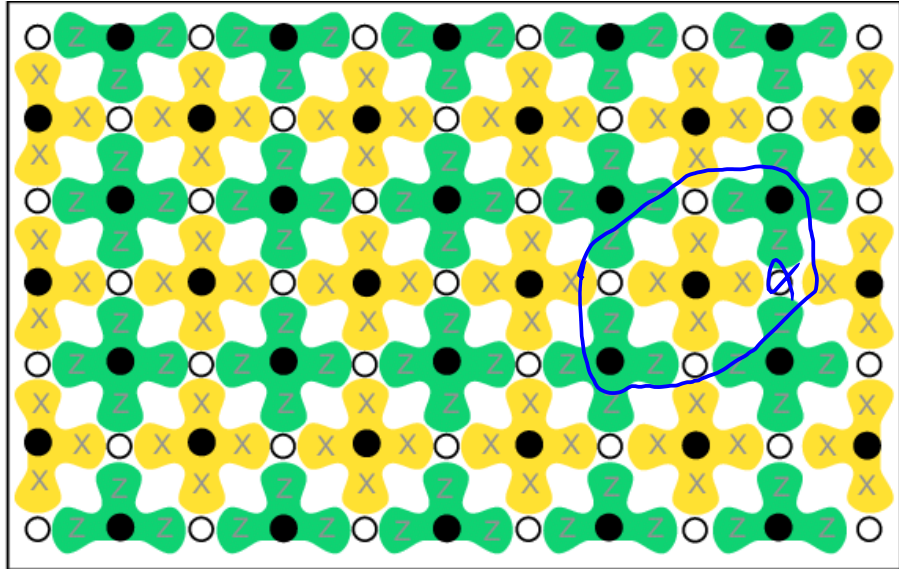
Similarly \swarrow error on qubit b

$$X_a X_b X_c X_d Z_b |\psi\rangle$$

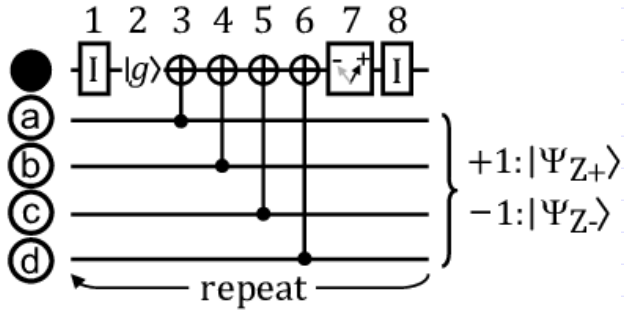
$$= -Z_b X_a X_b X_c X_d |\psi\rangle = -Z_b |\psi\rangle$$

P_e
 $P_{d/2}$
 $P_e()$
 $\sim d$
 Chains of errors
 $\sim d/2$

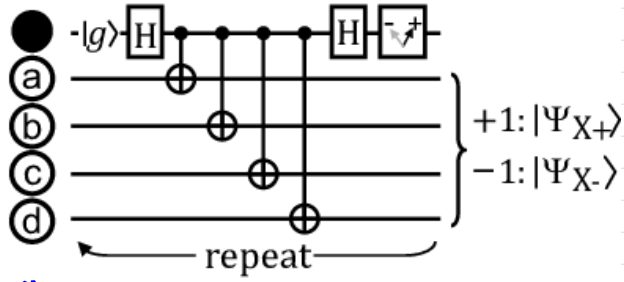
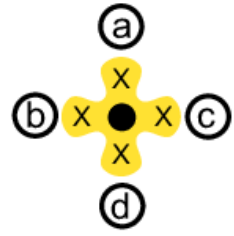
(a)



(b)



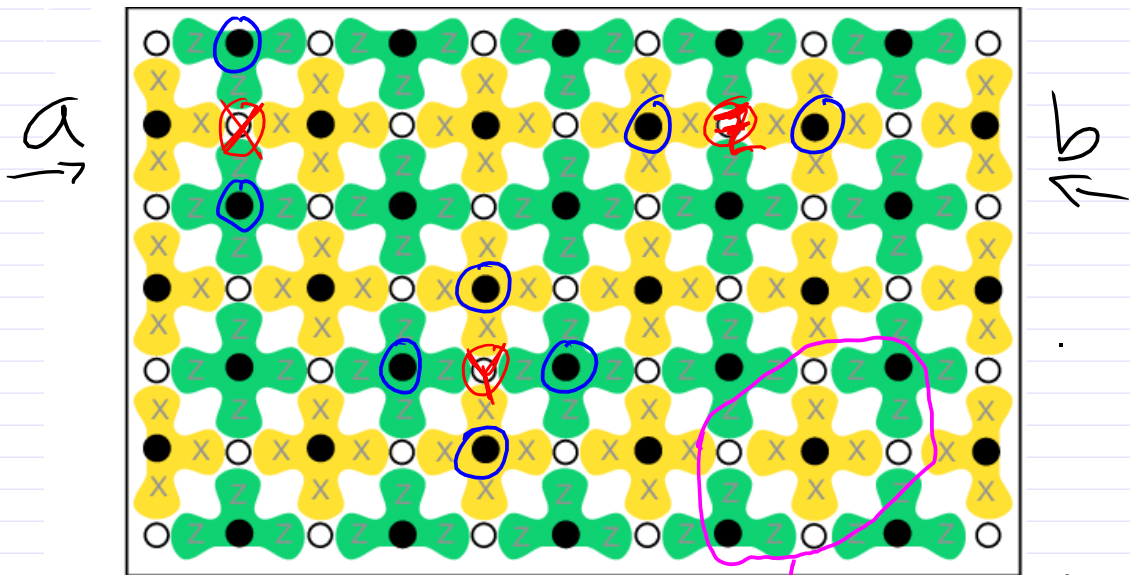
(c)



arXiv: 1208.0928

\bigcirc = flipped measurement value

\bigcirc = error on data qubit



$a = X$ error

$b = Z$ error

$c = Y$ error

39 \bigcirc "data"

38 \bigcirc "meas"

2d or 1 qubit

Repeated Quantum Error Detection in a Surface Code

Christian Kraglund Andersen,^{1,*} Ants Remm,¹ Stefania Lazar,¹ Sebastian Krinner,¹
 Nathàn Lacroix,¹ Graham J. Norris,¹ Mihai Gabureac,¹ Christopher Eichler,¹ and Andreas Wallraff¹

¹Department of Physics, ETH Zurich, CH-8093 Zurich, Switzerland

(Dated: December 20, 2019)

The realization of quantum error correction is an essential ingredient for reaching the full potential of fault-tolerant universal quantum computation. Using a range of different schemes, logical qubits can be redundantly encoded in a set of physical qubits. One such scalable approach is based on the surface code. Here we experimentally implement its smallest viable instance, capable of repeatedly detecting any single error using seven superconducting qubits, four data qubits and three ancilla qubits. Using high-fidelity ancilla-based stabilizer measurements we initialize the cardinal states of the encoded logical qubit with an average logical fidelity of 96.1%. We then repeatedly check for errors using the stabilizer readout and observe that the logical quantum state is preserved with a lifetime and coherence time longer than those of any of the constituent qubits when no errors are detected. Our demonstration of error detection with its resulting enhancement of the conditioned logical qubit coherence times in a 7-qubit surface code is an important step indicating a promising route towards the realization of quantum error correction in the surface code.

1912.09410

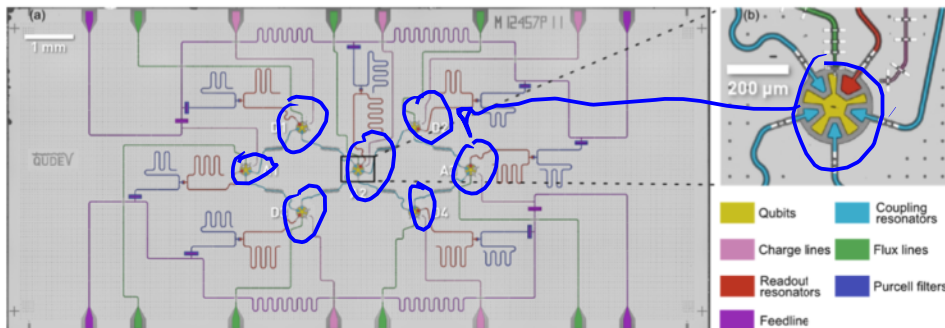
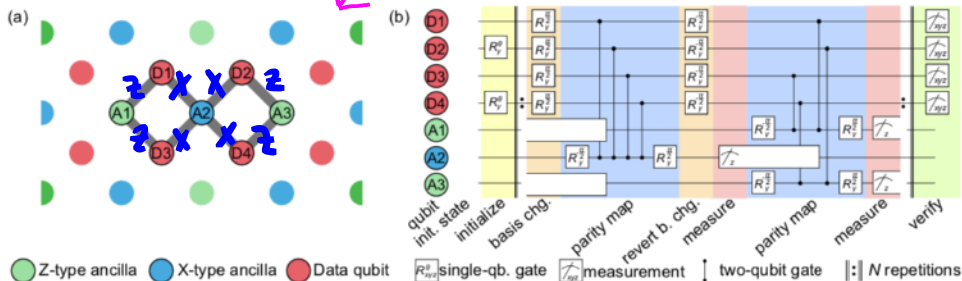


FIG. 2. Seven-qubit device. (a) False colored micrograph of the seven-qubit device used in this work. Transmon qubits are shown in yellow, coupling resonators in cyan, flux lines for single-qubit tuning and two-qubit gates in green, charge lines for single-qubit drive in pink, the two feedlines for readout in purple, transmission line resonators for readout in red and Purcell filters for each qubit in blue. (b) Enlarged view of the center qubit (A2) which connects to four neighboring qubits.

In the surface code, as in any stabilizer code, errors are detected by observing changes in the stabilizer measurement outcomes. Such syndromes are typically measured by entangling the stabilizer operators with the state of ancilla qubits, which are then projectively measured to yield the stabilizer outcomes. The surface code consists of a $d \times d$ grid of data qubits with $d^2 - 1$ ancilla qubits, each connected to up to four data qubits [28]. The code can detect $d - 1$ errors and correct up to $\lfloor (d - 1)/2 \rfloor$ errors per cycle of stabilizer measurements. In particular, the stabilizers of the $d = 2$ surface code, see Fig. 1 are given by

$$\begin{matrix} A_2 & A_1 & A_3 \\ X_{D1}X_{D2}X_{D3}X_{D4}, & Z_{D1}Z_{D3}, & Z_{D2}Z_{D4}. \end{matrix} \quad (1)$$

For the code-distance $d = 2$, it is only possible to detect a single error per round of stabilizer measurements and once an error is detected, the error can not be unambiguously identified, e.g. one would obtain the same syndrome outcome for an X -error on D1 and on D3.

Here, we use the following logical qubit operators

$$Z_L = Z_{D1}Z_{D2}, \quad \text{or} \quad Z_L = Z_{D3}Z_{D4}, \quad (2)$$

$$X_L = X_{D1}X_{D3}, \quad \text{or} \quad X_L = X_{D2}X_{D4}, \quad (3)$$

such that the code space in terms of the physical qubit states is spanned by the logical qubit states

$$\rightarrow |0\rangle_L = \frac{1}{\sqrt{2}}(|0000\rangle + |1111\rangle), \quad (4)$$

$$\rightarrow |1\rangle_L = \frac{1}{\sqrt{2}}(|0101\rangle + |1010\rangle). \quad (5)$$

$= X_L |0\rangle_L$

To encode quantum information in the logical subspace, we initialize the data qubits in a separable state, chosen such that after a single cycle of stabilizer measurements and conditioned on ancilla measurement outcomes being $|0\rangle$, the data qubits are encoded into the target logical qubit state. In this work, we demonstrate this probabilistic preparation scheme for the logical states $|0\rangle_L, |1\rangle_L, |+\rangle_L = (|0\rangle_L + |1\rangle_L)/\sqrt{2}$ and $|-\rangle_L = (|0\rangle_L - |1\rangle_L)/\sqrt{2}$ and we perform repeated error detection on these states.

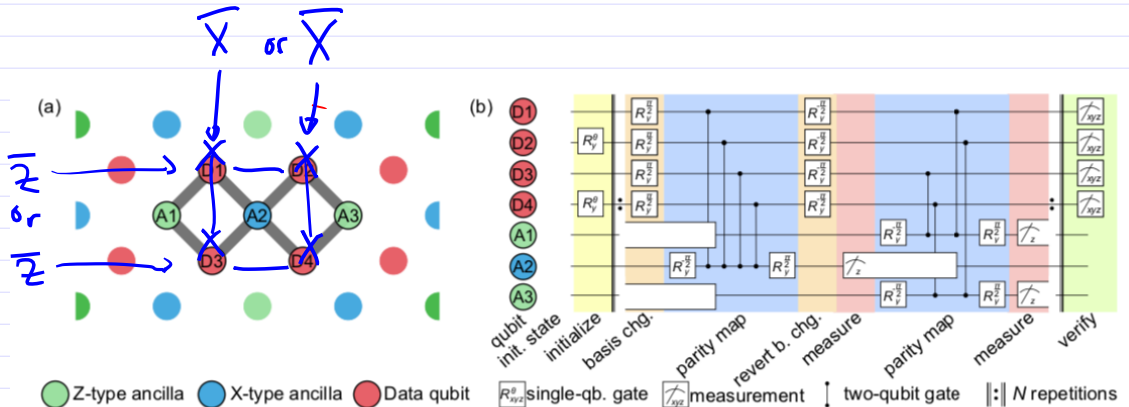


FIG. 1. Seven qubit surface code. (a) The surface code consists of a two-dimensional array of qubits. Here the data qubits are shown in red and the ancilla qubits for measuring X -type (Z -type) stabilizers in blue (green). The smallest surface code consists of seven qubits indicated by the data qubits D1-D4 and the ancilla qubits A1-A3. (b) Gate sequence for quantum error detection using the seven qubit surface code. Details of the gate sequence are discussed in the main text.

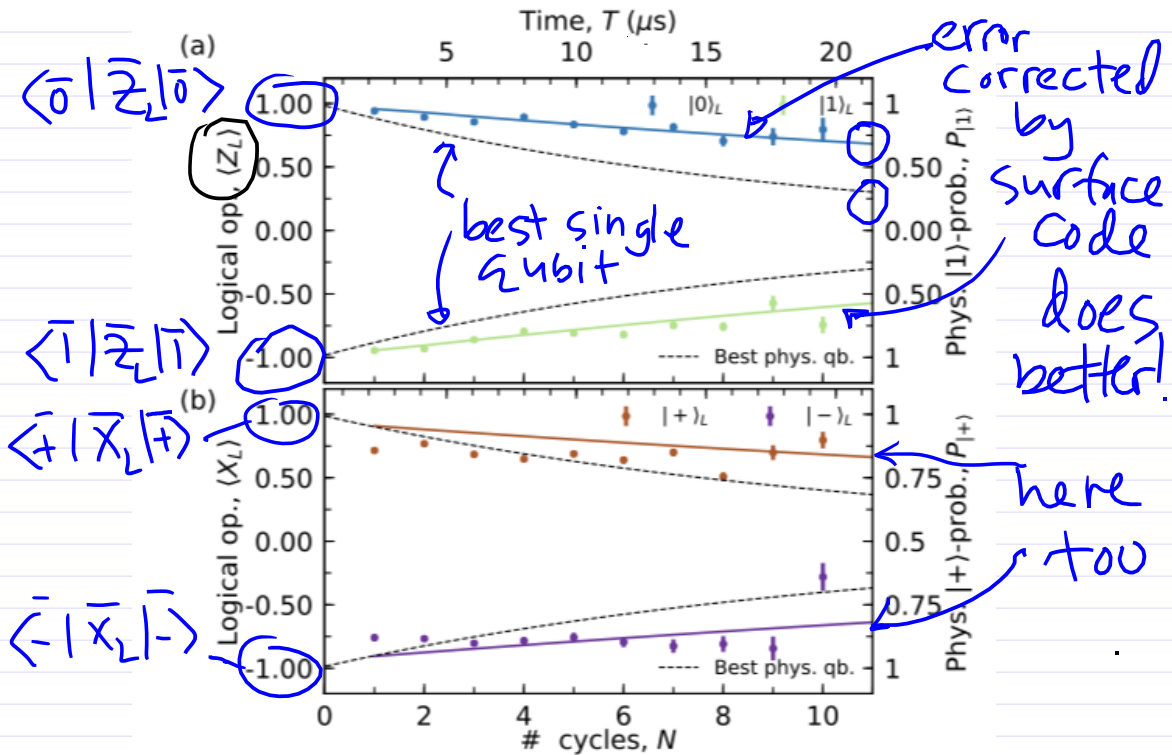
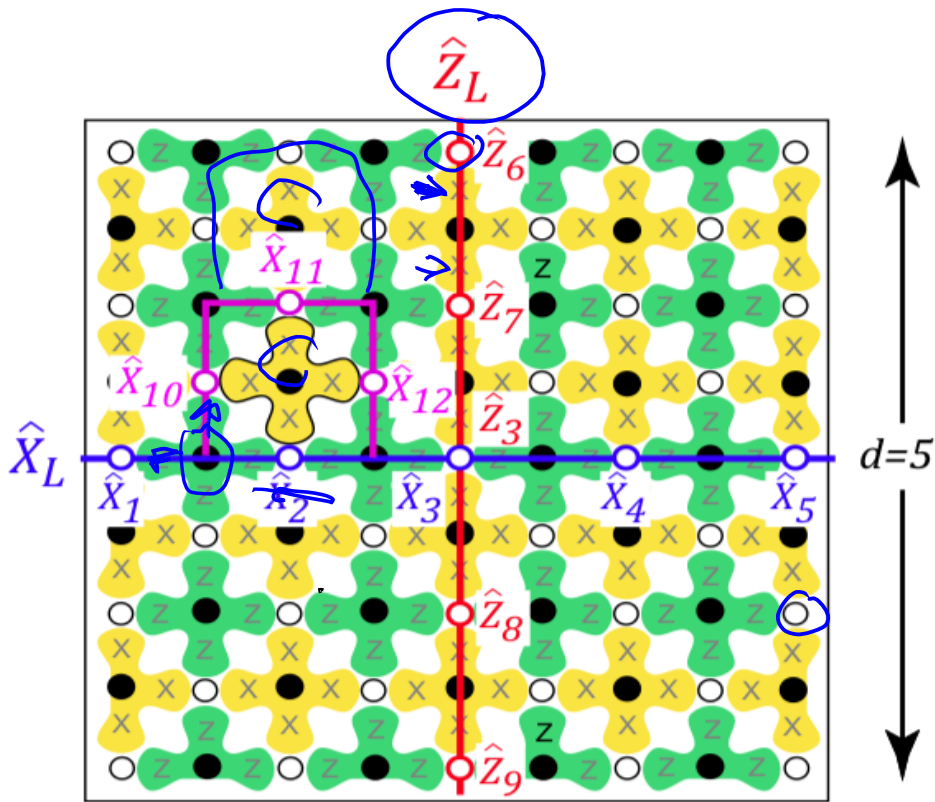
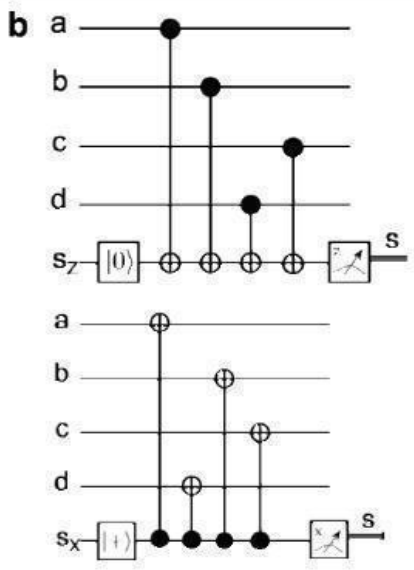
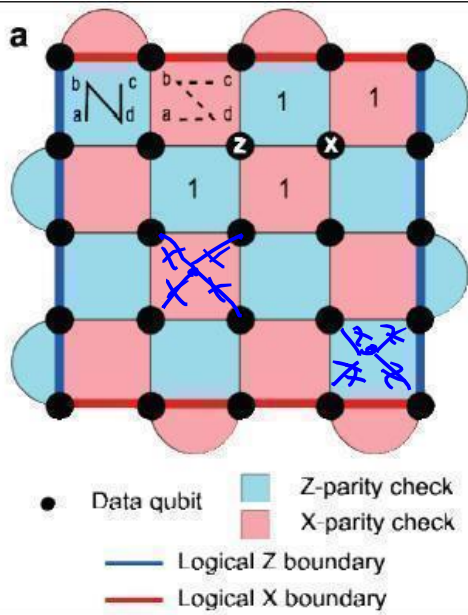


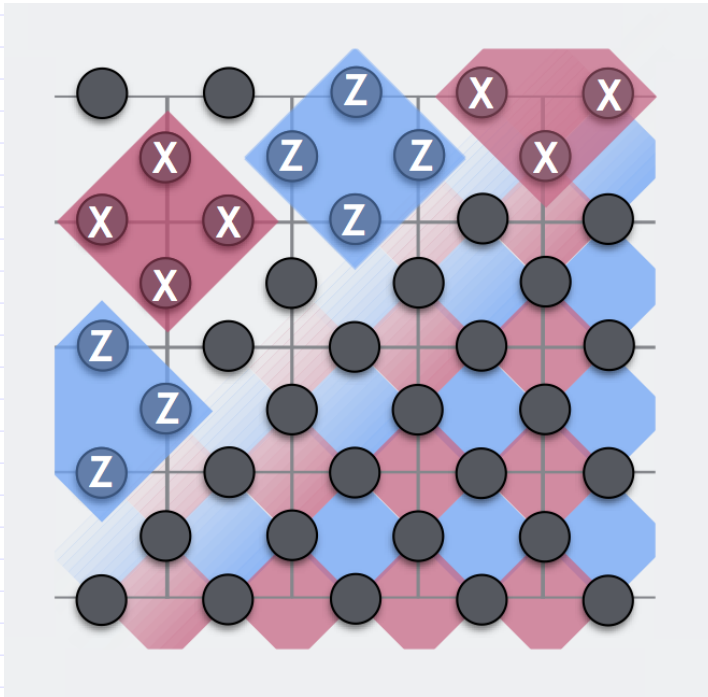
FIG. 5. Repeated quantum error detection. The expectation values of (a) the logical Z_L operator and (b) the logical X_L operator as a function of N , the number of stabilizer measurement cycles. The expectations values are shown for the prepared $|0\rangle_L$ (blue), $|1\rangle_L$ (green), $|+\rangle_L$ (brown) and $|-\rangle_L$ (purple) states. The solid lines indicate the corresponding values obtained from master equation simulations. Also shown (dashed lines, right axis) are the (a) qubit decay of the $|1\rangle$ -state with the best measured T_1 value and (b) the physical qubit decay of the $|+\rangle$ -state with the best measured T_2 value. (c) Total success probability p_s for detecting no errors during N cycles of stabilizer measurements for the $|0\rangle_L$ data shown in (a) and the corresponding values from numerical simulations. (d) Probability of observing k ancilla qubits in the $|1\rangle$ state for each measurement cycle and conditioned on having detected no error in any of the previous $N-1$ cycles. The data corresponds to the initial $|0\rangle_L$ state presented in (a).



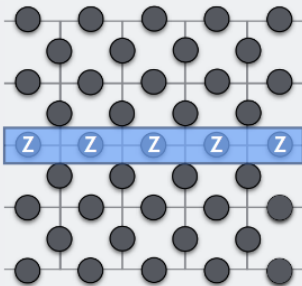
Still need logical operators
 \bar{X}_L, \bar{Z}_L satisfying
 $\bar{X}_L^2 = \bar{Z}_L^2 = 1, \quad \bar{X}_L \bar{Z}_L = -\bar{Z}_L \bar{X}_L$



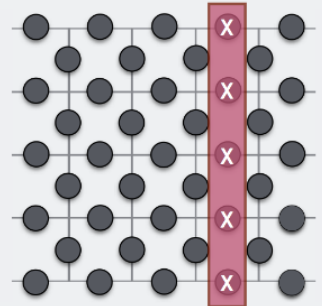
(IBM group)

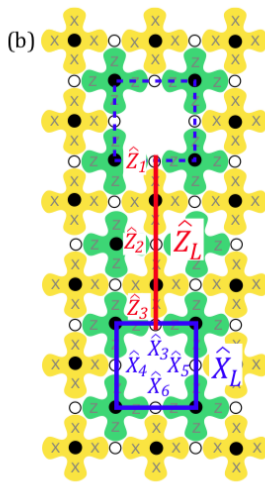
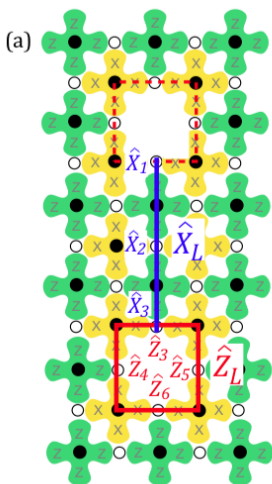
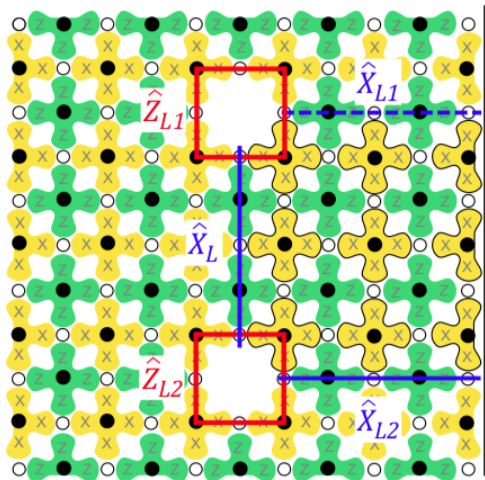
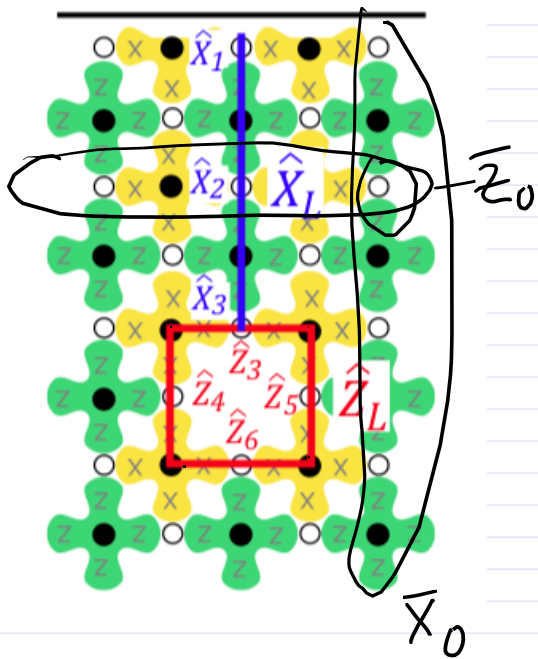


- logical **Z** operator:



- logical **X** operator:





Quantum Physics

[Submitted on 24 Aug 2024]

Quantum error correction below the surface code threshold

Quantum error correction provides a path to reach practical quantum computing by combining multiple physical qubits into a logical qubit, where the logical error rate is suppressed exponentially as more qubits are added. However, this exponential suppression only occurs if the physical error rate is below a critical threshold. In this work, we present two surface code memories operating below this threshold: a distance-7 code and a distance-5 code integrated with a real-time decoder. The logical error rate of our larger quantum memory is suppressed by a factor of $\Lambda = 2.14 \pm 0.02$ when increasing the code distance by two, culminating in a 101-qubit distance-7 code with $0.143\% \pm 0.003\%$ error per cycle of error correction. This logical memory is also beyond break-even, exceeding its best physical qubit's lifetime by a factor of 2.4 ± 0.3 . We maintain below-threshold performance when decoding in real time, achieving an average decoder latency of $63 \mu\text{s}$ at distance-5 up to a million cycles, with a cycle time of $1.1 \mu\text{s}$. To probe the limits of our error-correction performance, we run repetition codes up to distance-29 and find that logical performance is limited by rare correlated error events occurring approximately once every hour, or 3×10^9 cycles. Our results present device performance that, if scaled, could realize the operational requirements of large scale fault-tolerant quantum algorithms.

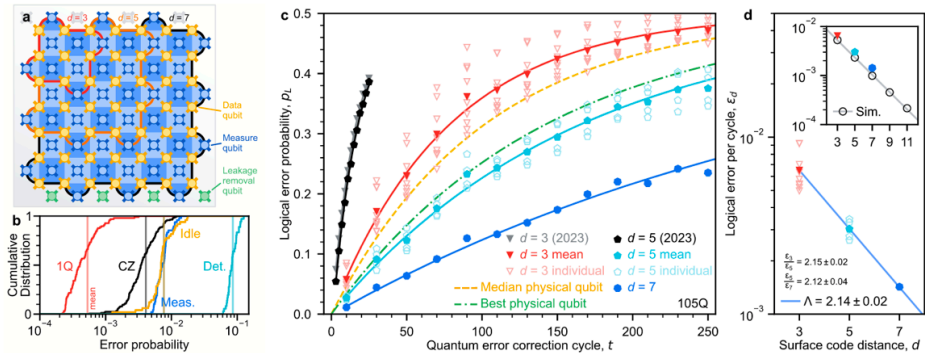


FIG. 1. Surface code performance. **a**, Schematic of a distance-7 surface code on a 105-qubit processor. Each measure qubit (blue) is associated with a stabilizer (blue colored tile). Red outline: one of nine distance-3 codes measured for comparison (3×3 array). Orange outline: one of four distance-5 codes measured for comparison (4 corners). Black outline: distance-7 code. We remove leakage from each data qubit (gold) via a neighboring qubit below it, using additional leakage removal qubits at the boundary (green). **b**, Cumulative distributions of error probabilities measured on the 105-qubit processor. Red: Pauli errors for single-qubit gates. Black: Pauli errors for CZ gates. Blue: Average identification error for measurement. Gold: Pauli errors for data qubit idle during measurement and reset. Teal: weight-4 detection probabilities (distance-7, averaged over 250 cycles). **c**, Logical error probability, p_L , for a range of memory experiment durations. Each datapoint represents 10^5 repetitions decoded with the neural network and is averaged over logical basis (X_L and Z_L). Black and grey: data from Ref. [17] for comparison. Curves: exponential fits after averaging p_L over code and basis. To compute ϵ_d values, we fit each individual code and basis separately [24]. **d**, Logical error per cycle, ϵ_d , reducing with surface code distance, d . Uncertainty on each point is less than 5×10^{-5} . Symbols match panel c. Means for $d = 3$ and $d = 5$ are computed from the separate ϵ_d fits for each code and basis. Line: fit to Eq. 1, determining Λ . Inset: simulations up to $d = 11$ alongside experimental points, both decoded with ensembled matching synthesis for comparison. Line: fit to simulation, $\Lambda_{\text{sim}} = 2.25 \pm 0.02$.